DIPOLAR NMR RELAXATION OF NONPROTONATED AROMATIC CARBONS IN PROTEINS

Structural and Dynamical Effects

RONALD M. LEVY
Department of Chemistry, Rutgers University, New Brunswick, NJ 08903

CHRISTOPHER M. DOBSON
Inorganic Chemistry Laboratory, South Parks Road, Oxford, England

MARTIN KARPLUS
Department of Chemistry, Harvard University, Cambridge, Massachusetts 02138

ABSTRACT The crystal structure and a 96-ps molecular dynamics simulation are used to analyze structural and motional contributions to spin-lattice (T_1) relaxation times of phenylalanine and tyrosine C^γ carbons of the pancreatic trypsin inhibitor. The H^β and H^δ protons geminal to C^γ are calculated to account for ~80% of the dipolar relaxation for each residue. Experimental T_1 values for the phenylalanine residues obtained at 25 MHz are observed to be 15–25% longer than estimates based on the rigid crystal structure. It is shown how an increase in T_1 can be related to order parameters for the picosecond motional averaging of the important C,H dipolar interactions, and how these order parameters can be calculated from a protein molecular dynamics trajectory.

INTRODUCTION

NMR relaxation measurements can provide both structural and dynamical information about proteins (1–4). To date, most NMR studies of internal motions in proteins have utilized proton-decoupled ^{13}C NMR methods (5–17). Protonated carbons in particular have been studied because the relaxation is dominated by the fluctuating dipolar interactions between ^{13}C nuclei and directly bonded protons (18, 19). Because dipolar relaxation is efficient for these carbons and the protonated carbon region of the spectrum is already crowded, there often result broad overlapping resonances and formidable resolution problems; nevertheless, important studies of relaxation effects have been made for protonated carbons. Nonprotonated carbon resonances are attractive for study because they are relatively few in number, and because the line widths are narrow at low field due to the larger distances between these carbons and the surrounding protons involved in the dipolar relaxation. Further, efficient double resonance techniques have been developed to select for nonprotonated carbon resonances both in solution (8, 20) and in the solid state (21). It will therefore soon be possible to compare solution and solid-state NMR studies of protein motions. For such an investigation the aromatic nonprotonated carbon resonances are particularly useful (8, 22, 23). Difficulties do arise, however, with the interpretation of the relaxation data for nonprotonated carbons, because a number of protons contribute to the dipolar relaxation and because additional relaxation mechanisms, such as chemical shift anisotropy, become important at higher magnetic fields. To aid in the interpretation of nonprotonated carbon data, a theoretical analysis of the structural and dynamic contributions to their relaxation is required.

In this paper we review the formulation of dipolar relaxation in terms of correlation functions that are determined by fluctuations in both the orientation of, and the distance between, both bonded and nonbonded $^{13}C,H$ atom pairs. For spectrometer frequencies below 45 MHz, ^{13}C spin relaxation is dominated by the dipole contribution. We focus on the γ-carbons of the four phenylalanines in the pancreatic trypsin inhibitor (PTI) because these resonances are relatively well resolved and because aromatic ring librational motions are particularly well suited for study using picosecond protein molecular dynamics methods. The PTI crystal structure and data from a 96-ps molecular dynamics simulation are used to evaluate structural and motional contributions to the spin lattice relaxation times (T_1 values) of these resonances. Corresponding results for the relaxation of the four tyrosine γ-carbons in PTI are also reported. The present study is an extension of the previous analysis of the effect of picosecond motional averaging on the ^{13}C NMR relaxation of protonated

carbons in PTI (24, 25). For the protonated carbons, only directly bonded protons need to be included in the relaxation mechanism; for the nonprotonated carbons we have to evaluate the contribution to the relaxation of all surrounding protons whether or not they are directly bonded. The picosecond motional averaging of the carbon-proton internuclear distances and angular orientations are calculated from the 96-ps trajectory and the effects of this averaging on the ^{13}C T_1 values are determined. The calculations for the phenylalanine γ-carbons are then compared with the measured T_1 values reported here.

THEORETICAL ANALYSIS OF RELAXATION

Method

The dipolar relaxation of ^{13}C nuclei in proteins is equal to the sum of the contributions from each of the surrounding protons; that is,

$$1/T_1 = \sum_j 1/T_{1j}. \quad (1)$$

For protonated carbons, the directly bonded contribution is dominant; for nonprotonated carbons it is necessary to sum over all near-carbon neighbors. In Eq. 1, $1/T_{1j}$ is the relaxation rate due to the dipolar interaction with the j^{th} proton (26),

$$1/T_{1j} = B\,[K_j^0(\omega_C-\omega_H) + 3K_j^1(\omega_C) + 6K_j^2(\omega_C+\omega_H)]. \quad (2)$$

The constant B has the value $(\gamma_C\gamma_H\hbar^2 4\pi/10)$; γ_C, γ_H, and ω_C, ω_H are the gyromagnetic ratios and Larmor frequencies of the ^{13}C and ^1H nuclei, respectively. The spectral densities have the form

$$K_j^m(\omega) = \int_0^\infty \left\langle \frac{Y_m^2(\Omega_j(t))\; Y_m^{2*}(\Omega_j(0))}{r_j^3(t)\, r_j^3(0)} \right\rangle \cos\omega t\, dt \quad (3)$$

where $Y_m^2(\Omega_j(t))$ is a second-order spherical harmonic; the angle Ω_j specifies the orientation with respect to the external magnetic field, of the internuclear vector from the relaxing carbon to the j^{th} proton. From Eq. 3 it is clear that the fluctuations in internuclear distances can provide a relaxation mechanism (27–29), in addition to the usually considered reorientation effect (15–19). For a rigid, isotropically tumbling protein, the spectral density at frequency ω arising from the dipolar interaction of a ^{13}C nucleus with a single proton j is

$$K_j^m(\omega) = \frac{\langle |[Y_m^2(0)]|^2 \rangle}{r_j^6} \frac{\tau_0}{1+(\omega\tau_0)^2}, \quad (4)$$

where τ_0 is the rotational correlation time for the protein and $\langle |[Y_m^2(0)]|^2 \rangle = 1/4\pi$. From Eq. 1–3, the total dipolar relaxation rate for a nonprotonated carbon in a rigid protein is

$$\frac{1}{T_1^R} = B\sum_j \frac{\langle |[Y_m^2(0)]|^2 \rangle}{r_j^6} \times \left[\frac{\tau_0}{1+(\omega_H-\omega_C)^2\tau_0^2} + \frac{3\tau_0}{1+\omega_C^2\tau_0^2} + \frac{6\tau_0}{1+(\omega_H+\omega_C)^2\tau_0^2} \right]. \quad (5)$$

For the specific case of aromatic C^γ carbons, the four protons (H^β and H^δ) on the same residue are expected to provide the major source of the relaxation; (see Fig. 1) previous quantitative studies have considered only the protons two and three bonds removed on the same ring (5). Because the van der Waals distance of closest approach between an aromatic carbon and a proton is ~2.5 Å, additional protons could contribute significantly to the relaxation so that an investigation of the full sum in Eq. 5 is important even in the rigid limit.

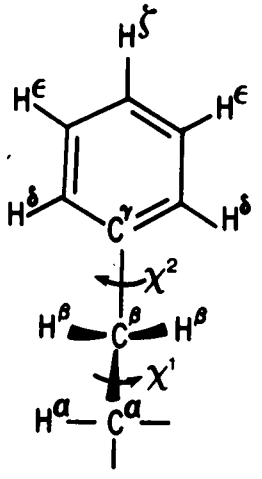

FIGURE 1 Structure of the phenylalanine side chain.

In spite of the close-packed structure of native proteins, significant motions (e.g., ring librations) occur on a picosecond time scale (1, 3, 30–32). In the presence of such motions the spectral density contributing to the NMR relaxation no longer has the form of Eq. 4. To evaluate the effect of internal protein motions on T_1, it is convenient to separate the NMR time correlation functions (Eq. 3) into contributions from protein tumbling and internal motions (33–35); with this approximation and the transformation properties of spherical harmonics, the integrand of Eq. 3 becomes

$$\left\langle \frac{Y_m^2(\Omega_j(t))\; Y_m^{2*}(\Omega_j(0))}{r_j^3(t) r_j^3(0)} \right\rangle = \sum_{aa'} \langle D_{ma}^2(\Omega_{LD}(t)) D_{ma'}^{2*}(\Omega_{LD}(0)) \rangle \left\langle \frac{Y_a^{2*}(\theta_j(t)\phi_j(t))\; Y_{a'}^2(\theta_j(0)\phi_j(0))}{r_j^3(t) r_j^3(0)} \right\rangle. \quad (6)$$

The D_{ab}^2 are Wigner rotation matrix elements (36), (Ω_{LD} are the Euler angles that transform from the laboratory fixed frame to a protein diffusion frame, and the time-dependent spherical polar coordinates $(\theta_j(t)\phi_j(t))$ are the spherical polar coordinates of the C^γ,H^j internuclear vector with respect to an arbitrary coordinate frame (e.g., the diffusion frame) tumbling rigidly with the protein. For an isotropically tumbling protein the time correlation function for the protein tumbling decays as a single exponential (30),

$$\langle D_{ma}^2(\Omega_{LD}(t))\, D_{ma'}^{2*}(\Omega_{LD}(0)) \rangle = \frac{e^{-t/\tau_0}}{5}\delta_{aa'}. \quad (7)$$

Introducing Eq. 7 into Eq. 6 we have

$$\left\langle \frac{Y_m^2(\Omega_j(t)) Y_m^{2*}(\Omega_j(0))}{r_j^3(t) r_j^3(0)} \right\rangle = e^{-t/\tau_0}/5 \sum_a \left\langle \frac{Y_a^2(\theta_j(t)\phi_j(t))\; Y_a^{2*}(\theta_j(0)\phi_j(0))}{r_j^3(t) r_j^3(0)} \right\rangle. \quad (8)$$

Eq. 8 provides the basis for calculating the effect of picosecond internal motions on NMR relaxation of nonprotonated carbons from a molecular dynamics simulation. The time-correlation functions on the left side of Eq. 8 depend on both the internal protein motions and the protein tumbling, while on the right hand side the tumbling contribution has been factored out and the spherical harmonics time-correlation functions depend only on the internal motions. Because of the highly restricted

nature of the motion in the protein interior, the internal correlation functions generally do not decay to zero. Instead a plateau value is often reached after t_p ps, where t_p is a short time compared with the length of the trajectory and $t_p\omega << 1$ (24, 25). For such a plateau value, the internal correlation function is equal to the equilibrium orientation distribution (25, 34) obtained from the entire run,

$$\frac{4\pi}{5}\sum_a \left| \left\langle \frac{Y_a^2(\theta_j(t)\phi_j(t))}{r_j^3(t)} \right\rangle \right|^2 = (\mathcal{S}_j)^2 \times \langle r^{-6} \rangle . \qquad (9)$$

The quantity $\mathcal{S}_j$ defined by Eq. 9 is the generalized order parameter for the restricted motion of the C^γ,H^j vector (37)[1]; for a rigid system $\mathcal{S}_j = 1$. Angular averaging of the spherical harmonics decreases the order parameter, as does radial averaging because the distance dependence of the order parameter is proportional to $\langle r^{-3} \rangle / \langle r^{-6} \rangle^{1/2}$. $\mathcal{S}_j$ is closely related to the order parameter that describes motional narrowing of deuterium quadrupole splittings in partially ordered systems. For the cylindrically symmetric case, the order parameter is defined (38) as

$$S_j = \langle P_2(\cos(\theta_j)) \rangle, \qquad (10)$$

where θ_j is the angle between the symmetry axis of the system and the C—D bond, and P_2 is an associated Legendre polynomial. For C^γ,H^j pairs where distance fluctuations are insignificant and motion of the internuclear vector is axially symmetric, $S_j = \mathcal{S}_j$.

Combining Eqs. 2, 3, and 9 we see that the carbon relaxation corrected for the picosecond motional averaging of the C^γ,H^j internuclear vector is

$$T_{1j} = (\mathcal{S}_j)^{-2} T_{1j}^R, \qquad (11)$$

where the rigid relaxation time, T_{1j}^R is calculated from Eqs. 2 and 4. Because $\mathcal{S}_j$ is ≤ 1, T_{1j} is larger than T_{1j}^R The generalized order parameter correction (Eq. 11) can be used independent of spectrometer frequency, because picosecond protein motions decrease spectral densities at all accessible Larmor frequencies uniformly. Levy et al. (25) have previously evaluated corrections to T_1^R for protonated carbons, which were called motional averaging scale factors. From Eq. 11 it is apparent the motional averaging scale factor is just the inverse of the square of the order parameter. The difference between the previous and present case is that for protonated carbons the vibrational averaging of the C—H bond lengths could be ignored, while for the nonbonded (C,H) interactions distance fluctuations can play a significant role.

Static C,H distances were evaluated using the refined x-ray crystal structure of Diesenhofer and Steigemann (39). Proton coordinates were generated from the heavy atom positions using a program adapted by Jeff Hoch (Harvard University) from one supplied by H. J. C. Berendsen (University of Groningen). Motional averaging of internuclear distances and order parameters were calculated from a 96-ps PTI molecular dynamics trajectory (30); a total of 653 coordinate sets spaced at 0.147-ps intervals were used in the calculation. To generate the simulation, the refined PTI crystal structure was energy minimized and brought to a temperature of 300 K over an equilibration period of 75 ps; this was followed by a 96-ps simulation, which provided the portion of the trajectory used for statistical analysis. The average temperature during this period was 300 K. Additional details concerning the trajectory have been reported previously (30).

Results of Calculations

Because the proton contribution to the relaxation rate of a C^γ aromatic carbon is to a first approximation proportional to $\Sigma_j(r_j^{-6})$, we show in Table I the values of this quantity determined from the crystal structure and the results obtained by averaging over the molecular dynamics trajectory. The static results for the four carbons are essentially the same; they are 0.054 ± 0.002 Å^{-6}. Using Phe 4 as an example, we list in Table II all protons within 4 Å of C^γ. From the crystal structure, the four geminal protons (H^δ,H^β) are calculated to account for ~80% of the relaxation, the other intraresidue protons provide ~10% of the relaxation, while all (366) protons on other residues contribute an additional ~10%. Similar results are obtained for all the phenylalanine and tyrosine carbons.

Dynamic averaging of the internuclear distances is seen (Table I) to have a very small effect on $\Sigma_j\langle r_j^{-6} \rangle$ values. The geminal (H^β and H^δ) protons still provide 80% of the relaxation. Fluctuations in the bond length and angle coordinates that determine the internuclear distances for these pairs are so restricted that the average distance distributions are well approximated by the crystal structure values (see below). Table II also compares distances of protons within 4 Å of Phe 4 C^γ from the crystal coordinates with values calculated from the first and last configurations of the 96-ps trajectory. Though geminal protons remain within 0.05 Å of crystal structure values, there are greater differences for the rest of the

TABLE I
INTERNUCLEAR DISTANCE CONTRIBUTION TO C^γ T_1 VALUES (Å^{-6})*

Residue	Crystal: $\Sigma_j\langle r_j^{-6} \rangle$	Dynamics: $\Sigma_j\langle r_j^{-6} \rangle$
Phe 4	0.055	0.053
Phe 22	0.054	0.053
Phe 33	0.052	0.055
Phe 45	0.054	0.058

*All protons within 4 Å of C^γ included in the sum. The contribution from protons two bonds removed from C^γ (H^β and H^δ protons) is 0.046 Å^{-6}.

TABLE II
INTERNUCLEAR DISTANCES FROM PHE 4 C^γ TO NEIGHBORING PROTONS

	Internuclear distance*		
	Crystal	First configuration	Last configuration
Phe 4 protons			
$H^{\delta 1}$ Phe 4	2.10	2.05	2.11
$H^{\delta 2}$ Phe 4	2.12	2.17	2.14
$H^{\beta 1}$ Phe 4	2.10	2.14	2.14
$H^{\beta 2}$ Phe 4	2.10	2.14	2.14
$H^{\epsilon 2}$ Phe 4	3.39	3.49	3.44
$H^{\epsilon 1}$ Phe 4	3.40	3.41	3.49
H^ζ Phe 4	3.88	3.93	3.87
H^α Phe 4	3.46	3.44	3.48
H^N Phe 4	2.72	3.30	3.38
Protons on other residues			
$H^{\delta 2}$ Arg 42	3.19	>4.0	>4.0
$H^{\beta 2}$ Arg 42	3.23	>4.0	>4.0
$H^{\beta 1}$ Arg 42	3.37	>4.0	>4.0
$H^{\beta 1}$ Pro 2	3.29	>4.0	>4.0
H^N Cys 5	>4.0	2.19	2.70
$H^{\beta 1}$ Cys 5	>4.0	3.70	>4.0
H^N Leu 6	>4.0	>4.0	2.73
$H^{\gamma 2}$ Glu 7	>4.0	>4.0	3.31

*Distances in Å. The first configuration of the trajectory follows a 75-ps equilibration period.

[1]Lipari, G., and A. Szabo. A model-free approach to the interpretation of nuclear magnetic resonance in macromolecules. I. Theory and range of validity. *J. Am. Chem. Soc.* In press.

protons; all those in the same residue are still quite similar, except for the H^N distance which is significantly larger in the dynamics. Also of interest is the appearance of a proton (Cys 5 H^N) within the van der Waals diameter of the C^γ carbon of Phe 4 (first configuration of the trajectory). Such an event must be rare because there is close agreement between crystal structure and motionally averaged estimates of $\Sigma_j r_j^{-6}$ (Table I).

For each of the four Phe C^γ carbons, we have calculated the NMR correlation functions (Eq. 10) for dipolar relaxation by all protons on the same residue. The scale factors $(\mathcal{S}_j)^{-2}$, by which T_{1j}^R are increased, are listed in Tables III A and B. Table III A presents the results for relaxation by the ring protons H^δ, H^ϵ, H^ζ. For these dipole pairs, internuclear distance fluctuations make essentially no contribution to the relaxation; the averaging is due to angular reorientation of the internuclear vectors. We compare the scale factors estimated from the equilibrium expression, (Eq. 9) with a lower estimate obtained by replacing the equilibrium average with the value of the NMR correlation functions (Eq. 8) at short times (t = 2 ps). The correlation functions over 8 ps for dipolar interactions of Phe 4 C^γ with the ring protons are shown in Fig. 2. There is a rapid initial decay within the first 2 ps after which the correlation functions appear to be at a plateau value. This fast decay results from the motions determined by the combined effect of the potential for the side chain torsional angles χ^1 and χ^2 and collisions between the atoms of the ring and those of the surrounding cage in the protein (40). Considering the scale factors evaluated from the correlation function values at 2 ps in Table III A, the four phenylalanine rings exhibit qualitatively similar behavior for the picosecond dynamics. For each of the rings the greatest averaging occurs along the C^γ,H^δ direction with increases in T_{1j} ranging from 20% for Phe 33 and 45 to 80% for Phe 22; motional averaging is smallest along the C^γ,H^ζ direction.

For rings Phe 35 and 45, the dipolar relaxation results obtained at t = 2 ps from the correlation function (Eq. 8) and from the equilibrium average (Eq. 9) are essentially the same as expected if a plateau value is reached for the dynamics trajectory after 2 ps. By contrast for Phe 4 and 22 the motional averaging for selected dipole pairs is much greater when the equilibrium average (Eq. 9) is used to estimate the dipolar relaxation as compared with the 2 ps values of the correlation functions. The difference is due to the fact that the rings of Phe 4 and 22 each undergo one 180° flip during the simulation. This has a large effect on the equilibrium average due to the reorientation of the dipole vector produced by the ring flip.

For the rings that do not flip, Phe 33 and 45, a simple restricted diffusion model (35) for the ring motions does account for the dependence of the scale factors on the orientation of the dipole vectors in the ring plane. If the restricted diffusion is about the C^β–C^γ axis, the order parameter is smallest (the scale factor is greatest) along the C^γ,H^δ direction, and $(\mathcal{S}_j)^2$ = 1 along the C^γ—H^ζ direction because this vector lies directly on the diffusion axis. For all of the phenylalanine and tyrosine rings in PTI the order parameters for the C^γ,H^ζ dipolar interactions are calculated to be <1; this is due to additional motion about the side chain C^α–C^β axis. For the dipolar pairs listed for Phe 4 and 22 (Table III A), the dependence of the motional averaging on the orientation of the dipole vector in the ring plane is strongly affected by the ring flips of these two residues. The order parameters for these two rings calculated using both Eq. 8 and Eq. 9 have been fit to a restricted diffusion plus jump (ring flip) model for the ring motion[2]. For the dipolar pairs considered in Table III A, the greatest increase in motional averaging due to the jump is expected along the C^γ,H^ϵ direction, in agreement with the results calculated for Phe 4 and 22 (Table III A).

The scale factors obtained for the motional averaging of the C^γ dipolar interactions with the remaining phenylalanine protons (H^α, H^β, and H^N) are listed in Table III B. The values were obtained from the equilibrium expression (Eq. 10); essentially the same values were obtained from the short time (2 ps) decay of the correlation functions, indicating that the plateau value approximation is correct. The results obtained using the complete expression for the motional averaging are compared with the scale factors obtained when only angular fluctuations are considered. As expected, for the C^γ,H^β interactions, distance fluctuations make no contribution to the relaxation since the internuclear distance is determined by bond length and angle coordinates. Of the other dipole pairs, for which internuclear distances also depend on the dihedral angle, only for the C^γ,H^α pair of the Phe 45 do internuclear distance fluctuations increase the motional averaging by more than ~5%. It is of interest, therefore, to compare the dynamically averaged internuclear distances $\langle r_j \rangle$ listed in

TABLE IIIA
MOTIONAL AVERAGING OF PHENYLALANINE C^γ DIPOLAR INTERACTIONS WITH RING PROTONS

Nuclear dipole pair		Motional averaging scale factor	
Carbon	Proton	t_p = 2 ps*	t_p = 96 ps‡
Phe 4 C^γ	$H^{\delta1}$	1.60	1.66
	$H^{\delta2}$	1.58	1.61
	$H^{\epsilon1}$	1.39	3.58
	$H^{\epsilon2}$	1.39	3.99
	H^ζ	1.20	1.21
Phe 22 C^γ	$H^{\delta1}$	1.82	3.21
	$H^{\delta2}$	1.77	2.97
	$H^{\epsilon1}$	1.42	3.31
	$H^{\epsilon2}$	1.40	3.28
	H^ζ	1.15	1.26
Phe 33 C^γ	$H^{\delta1}$	1.20	1.26
	$H^{\delta2}$	1.22	1.27
	$H^{\epsilon1}$	1.14	1.17
	$H^{\epsilon2}$	1.15	1.17
	H^ζ	1.11	1.13
Phe 45 C^γ	$H^{\delta1}$	1.20	1.28
	$H^{\delta2}$	1.20	1.28
	$H^{\epsilon1}$	1.14	1.16
	$H^{\epsilon2}$	1.14	1.21
	H^ζ	1.10	1.14

TABLE IIIB
MOTIONAL AVERAGING OF PHENYLALANINE C^γ DIPOLAR INTERACTIONS WITH H^β AND BACKBONE PROTONS

Nuclear dipole pair		Internuclear distance			Motional averaging scale factor	
Carbon	Proton	Crystal	$\langle r \rangle$	$\langle r^{-6} \rangle^{1/6}$	Angular	Complete
					t_p = 96 ps§	t_p = 96 ps‡
Phe 4 C^γ	H^β		2.12	2.12	1.23	1.23
	H^α	3.46	3.14	3.07	1.08	1.09
	H^N	2.72	3.39	3.38	1.11	1.17
Phe 22 C^γ	H^β		2.12	2.12	1.42	1.42
	H^α	3.41	2.86	2.83	1.05	1.06
	H^N	3.05	4.07	4.02	1.05	1.12
Phe 33 C^γ	H^β		2.12	2.12	1.17	1.17
	H^α	3.39	3.43	3.42	1.05	1.06
	H^N	3.17	2.98	2.91	1.12	1.16
Phe 45 C^γ	H^β		2.12	2.12	1.28	1.30
	H^α	2.82	2.64	2.42	2.38	2.66
	H^N	3.45	3.53	3.48	1.05	1.09

*The motional averaging scale factor is T_{1j}/T_{1j}^R (Eq. 11) with $(\mathcal{S}_j)^{-2}$ approximated using the values at 2 ps of the NMR correlation functions (eq. 8).
‡$(\mathcal{S}_j)^{-2}$ calculated from Eq. 9.
§The motional averaging scale factor calculated from angular averaging alone, i.e., $(\mathcal{S}_j)^{-2} \approx 4\pi/5 \, \Sigma_a \left| \langle Y_a^2(\theta_j(t)\phi_j(t)) \rangle \right|^2$.

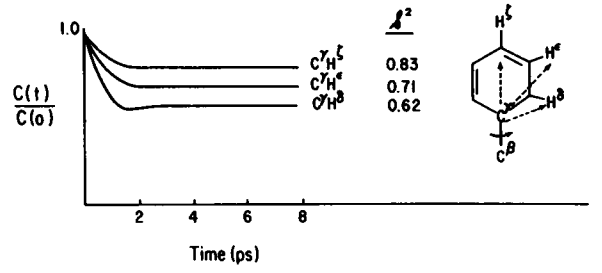

FIGURE 2 NMR correlation functions (Eq. 8 of text) for dipolar interactions of Phe 4 C^γ with H^δ, H^ϵ, and H^ζ ring protons. *Inset* shows numerical values of the order parameters. $\mathcal{S}^2$ obtained from the decay of the NMR correlation functions after 2 ps.

Table III B with the dipolar average $\langle r_j^{-6}\rangle^{-1/6}$, also presented in Table III B. Because $\langle r_j^{-6}\rangle$ dipolar averaging weights more heavily the fluctuations that bring the nuclear pair closer together, $\langle r_j^{-6}\rangle^{-1/6}$ is less than or equal to $\langle r_j\rangle$. The differences between the crystal structure value of r and $\langle r\rangle$ reflect differences between the average dynamics structure and the crystal structure. For the nuclear pairs considered in Table III B, the $\langle r_j\rangle$ are very close to the corresponding values $\langle r_j^{-6}\rangle^{-1/6}$, with the exception of the Phe 45 C^γ,H^α pair. These results provide additional support for the observation that picosecond internuclear distance fluctuations between C^γ aromatic carbons and surrounding protons have an effect that is small compared with the angular averaging of the dipole orientation. For cases where the specific interaction with protons distant along the polypeptide chains are important (e.g., Nuclear Overhauser Enhancement measurements), the r averaging will play a more important role.

To use the static and dynamic results presented above to evaluate T_1 for the C^γ carbons, a value for the rotational correlation time of PTI is required. Values have been reported that vary between 1.7 ns (10 mM PTI, 17°C [reference 13]) and 20 ns (50 mM PTI, 30° C [reference 10]). We use a value of 3.9 ns for the PTI rotational correlation time, which is the value reported under conditions similar to those used in the measurements described in the Experimental Measurements section (11). The calculated T_1 relaxation times are not very sensitive to the value chosen for the PTI rotational correlation time because at 25 MHz rigid protein T_1 values vary by <6% for rotational correlation times between 3–8 ns. The T_1 for each of the four Phe C^γ evaluated from Eq. 5 using the crystal structure geometry are listed in Table IV. The values are calculated to be close to 440 ms. That the variation in the predicted T_1 among the four carbons is small (~5%) is a consequence of the fact that the geminal (H^β,H^δ) protons dominate the relaxation. The corrections to the crystal structure T_1 predictions at 25 MHz obtained from the molecular dynamics simulation results are also listed in Table IV. T_1 values are reported from estimates of order parameters based on the decay of the NMR correlation functions at 2 ps and on the equilibrium expression for the order parameters (Eqs. 2, 8, and 9). The predicted increases in T_1 from picosecond motional averaging range from 10% (lower estimate for Phe 45) to almost 100% (upper estimate for Phe 22); the latter is certainly too high a value due to the occurrence of a ring flip in the trajectory (see Conclusions). Based on the decay of the NMR correlation functions at 2 ps, we find the average T_1 for the four phenylalanine γ-carbons to be 556 ms; this represents a 25% increase over the static result.

TABLE IV
CALCULATED T_1 VALUES OF PHENYLALANINE C^γ RESONANCES*

	Crystal	Dynamics	
Phe 4	434	599‡	618§
Phe 22	442	633	800
Phe 33	459	502	514
Phe 45	442	491	518
Mean	444	556	613

*Values in milliseconds. A rotational correlation time of 3.9 ns was assumed.
‡T_1 calculated from Eqs. 1 and 10; $(\mathcal{S}_j)^{-2}$ approximated using the values at 2 ps of the NMR correlation functions (Eq. 8).
§T_1 calculated from Eqs. 1 and 10; $(\mathcal{S}_j)^{-2}$ calculated from Eq. 9.

EXPERIMENTAL MEASUREMENTS OF T_1

Bovine pancreatic trypsin inhibitor (BPTI, Traysol, registered trademark of Farbenfabriken Bayer) was obtained as a gift from Bayer AG, Leverkusen, Federal Republic of Germany. 30-mM solutions of PTI in D_2O at pH 5.0 containing 0.1 mM EDTA were prepared. Oxygen was removed by several freeze-thaw cycles.

^{13}C NMR relaxation measurements were performed on the Varian XL-100 spectrometer (Varian Associates, Palo Alto, CA) at the Harvard Chemistry Department. The sample temperature in the probe with the decoupler on was maintained at 30°C. The longitudinal relaxation times were obtained using the standard 180°-τ-90° inversion recovery pulse sequence. Three separate experiments were made. For two of the experiments, seven partially relaxed Fourier transform (PRFT) spectra corresponding to delay times τ between 25 and 400 ms were obtained. Infinite time intensities were obtained from a one-pulse spectrum. 15,000 transients were accumulated for each PRFT spectrum with a recycle time of 2.0 s; total spectrometer time per spectrum was 8.3 h. In the third experiment 4 PRFT spectra were recorded with a recycle time of 3.4 s. No systematic differences between the experiments were observed. T_1 values were determined using a linear least-squares fit of the peak heights to the expression $\ln(A_\infty - A_\tau) = K - \tau/T_1$.

The aromatic region of the 25-MHz NMR spectrum of PTI is shown in Fig. 3. The four Phe C^γ resonances appear as two completely resolved resonances, and one two-carbon

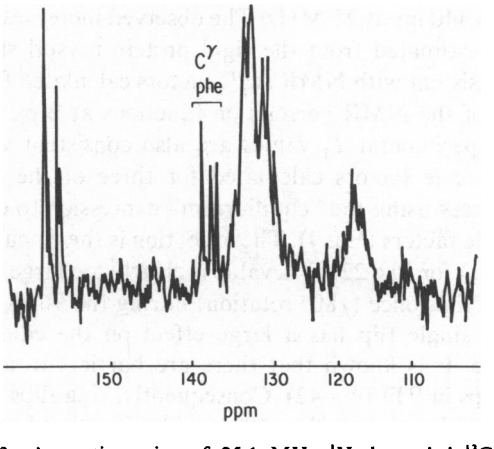

FIGURE 3 Aromatic region of 25.1 MHz ^1H decoupled ^{13}C NMR spectrum of 30 mM PTI showing the two carbon and the two one-carbon phenylalanine C^γ resonances.

resonance. The four Tyr C^{γ} resonances overlap with a broad band of protonated ring carbon resonances centered at 132 ppm. The average T_1 values and standard deviations obtained from the inversion recovery experiments are: 508 ± 10 ms, 521 ± 49 ms, and 553 ± 94 ms for the downfield (137.7 ppm), middle (136.5 ppm), and upfield (135.8 ppm) C^{γ} resonances, respectively. There is no indication of nonexponential behavior for any of the resonances, so that it may be concluded that the T_1 values for the C^{γ} involved are all close to the average value, 527 ms. The small variation suggests that the motions of all four phenylalanine rings of PTI are qualitatively similar.

CONCLUSIONS

The analysis of nonprotonated carbon dipolar NMR relaxation in PTI using a 96-ps molecular dynamics simulation has demonstrated how protein trajectories can be used to assess the effects on the relaxation of protein motions on the picosecond time scale. We have defined NMR scale factors and shown how to calculate them from protein trajectories. The scale factors are equal to the inverse of the square of the order parameters for the C,H dipole pairs and give the increase in T_1 values due to picosecond protein motions. Despite the bulky nature of aromatic rings and the restricted space available in the protein interior, the dynamics results show that the picosecond ring motions increase the relaxation times of nonprotonated ring carbon resonances. The protein motions are calculated to increase the C^{γ} relaxation times by 15–25% over the rigid structure values. For the dipolar interactions of the phenylalanine C^{γ} carbons with the surrounding phenylalanine protons, the decay of the NMR correlation functions is due to angular fluctuations in the orientation of the internuclear dipole vectors; internuclear distance fluctuations for these dipole pairs have a small effect on the relaxation.

For the three phenylalanine C^{γ} resonances, the average T_1 values measured from three separate inversion-recovery experiments vary between 508 and 553 ms at 25 MHz. The T_1 values calculated from the PTI crystal structure are close to 440 ms at 25 MHz. The observed increases over T_1 values estimated from the rigid protein crystal structure are consistent with NMR scale factors calculated from the decay of the NMR correlation functions at 2 ps (Eq. 8). The experimental T_1 values are also consistent with the NMR scale factors calculated for three of the four C^{γ} resonances using the "equilibrium" expression to evaluate the scale factors (Eq. 9). The exception is the calculated T_1 (800 ms) for Phe 22. This value is clearly too large because Phe 22 flips once (180° rotation) during the 96-ps simulation; a single flip has a large effect on the equilibrium average. It is known that there are barriers to aromatic ring flips in PTI (40–42). Consequently, ring flips are rare events with a time scale >100 ps. The fact that both Phe 4 and 22 flip during the simulation, must be regarded as an artifact of the single 96-ps trajectory used for the present analysis of NMR scale factors. The exact effect of flips on NMR relaxation of ring carbon resonances depends on several factors including the flip rate, the probe orientation, and the magnitude of the thermal oscillations of the ring about the equilibrium position.[2] Improved estimates of NMR scale factors for probes whose dynamics depend on both infrequent events and thermal oscillations require more extended trajectory simulations. Such an analysis has recently been carried out for the NMR relaxation of a model side chain attached to a macromolecule, where the computer simulations were carried out for times up to 100 ns (34).

We thank J. C. Hoch, E. T. Olejniczak, D. J. States, and A. Szabo for helpful discussions. We thank J. A. McCammon and J. Ramsdell for their contribution to calculating the 96-ps PTI trajectory. We thank H. Berendsen for supplying the program for generating protons in the extended atom model protein trajectory and J. C. Hoch for adapting the program.

This work has been supported by grants from the National Institutes of Health, the National Science Foundation, the Petroleum Research Fund administered by the American Chemical Society, and by the Rutgers University Research Council, and a Biomedical Research Support Grant.

Received for publication 1 September 1981 and in revised form 8 January 1982.

REFERENCES

1. Gurd, F. R. N., and M. Rothgeb. 1979. Motions in proteins. *Adv. Protein Chem.* 33:74–165.
2. Campbell, I. D., and C. M. Dobson. 1979. The application of high resolution nuclear magnetic resonance to biological research. *Methods Biochem. Anal.* 25:1–133.
3. Karplus, M., and J. A. McCammon. 1981. The internal dynamics of globular proteins. *CRC Crit. Rev. Biochem.* 9:293–349.
4. Wüthrich, K. 1976. NMR in Biological Research: Peptides and Proteins. North-Holland Publishing Co., Amsterdam. 1–376.
5. Oldfield, E., R. S. Norton, and A. Allerhand. 1975. Studies of individual carbon sites of proteins in solution by natural abundance carbon-13 nuclear magnetic resonance spectroscopy. *J. Biol. Chem.* 250:6368–6380.
6. Norton, R. S., A. O. Clouse, R. Addleman, and A. Allerhand. 1977. Studies of proteins in solution by natural abundance carbon-13 nuclear magnetic resonance. Spectral resolution and relaxation behavior at high magnetic field. *J. Am. Chem. Soc.* 99:79–83.
7. Dill, K., and A. Allerhand. 1977. Studies of individual methine aromatic carbon sites of proteins by natural abundance carbon-13 nuclear magnetic resonance spectroscopy at high magnetic field strengths. *J. Am. Chem. Soc.* 99:4508–4511.
8. Allerhand, A. 1978. Natural abundance carbon-13 nuclear magnetic resonance spectroscopy of proteins. Observations and uses of nonprotonated aromatic carbon resonances. *Accounts Chem. Res.* 11:469–474.
9. Dill, K., and A. Allerhand. 1979. Small errors in C—H bond lengths may cause large errors in rotational correlation times determined from carbon-13 spin lattice relaxation measurements. *J. Am. Chem. Soc.* 101:4376–4378.

[2]Levy, R. M. and R. Sheridan. Combined effect of restricted rotational diffusion plus jumps on probes of aromatic ring motions in proteins. *Biophys. J.* Submitted.

10. Wüthrich, K., and R. Baumann. 1976. ^{13}C spin relaxation studies of the basic pancreatic trypsin inhibitor. *Organic Magnetic Resonance.* 8:532–535.
11. Richarz, R., K. Nagayama, and K. Wüthrich. 1980. Carbon-13 nuclear magnetic resonance relaxation studies of internal mobility of the polypeptide chains in basic pancreatic trypsin inhibitor and a selectively reduced analogue. *Biochemistry.* 19:5189–5196.
12. Nelson, D. J., S. J. Opella, and O. Jardetzky. 1976. ^{13}C nuclear magnetic resonance study of molecular motions and conformational transitions in muscle calcium binding protein. *Biochemistry.* 15:5552–5560.
13. Ribeiro, A. A., R. King, C. Restivo, and O. Jardetzky. 1980. An approach to the mapping of internal motions in proteins. Analysis of ^{13}C NMR relaxation in the bovine pancreatic trypsin inhibitor. *J. Am. Chem. Soc.* 102:4040–4051.
14. Visscher, R., and F. R. N. Gurd. 1975. *J. Biol. Chem.* 250:2238–2242.
15. Wittebort, R. J., T. M. Rothgeb, A. Szabo, and F. R. N. Gurd. 1979. The aliphatic groups of sperm whale myoglobin. A ^{13}C NMR study. *Proc. Natl. Acad. Sci. U. S. A.* 76:1059–1066.
16. Jelinski, L. W., and D. Torchia. 1980. Investigation of labelled amino acid side chain motion in collagen using ^{13}C nuclear magnetic resonance. *J. Mol. Biol.* 138:255–272.
17. Howarth, O. W. 1978. Effect of internal librational motions on the ^{13}C NMR relaxation times of proteins and peptides. *J. Chem. Soc. Faraday Trans. II.* 74:1031–1040.
18. Kuhlmann, K. F., D. M. Grant, and R. K. Harris. 1970. Nuclear overhauser effects and ^{13}C relaxation times in ^{13}C—H double resonance spectra. *J. Chem. Phys.* 52:3439–3448.
19. Lyerla, J. R., Jr., and G. C. Levy. 1974. Carbon-13 nuclear spin relaxation. *In* Topics in Carbon 13 NMR Spectroscopy. 1:79–114.
20. Opella, S. J., and T. A. Cross. 1979. Enhanced selection of nonprotonated carbon resonances in solution NMR. *J. Magn. Res.* 37:171–175.
21. Opella, S. J., and M. H. Frey. 1979. Selection of nonprotonated carbon resonances in solid-state nuclear magnetic resonance. *J. Am. Chem. Soc.* 101:5854–5856.
22. Opella, S. J., M. H. Frey, and T. A. Cross. 1979. Detection and individual carbon resonances in solid proteins. *J. Am. Chem. Soc.* 101:5856–5857.
23. Opella, S. J., T. A. Cross, J. A. DiVerdi, and C. F. Sturm. 1980. Nuclear magnetic resonance of the filamentous bacteriophage fd. *Biophys. J.* 32:531–548.
24. Levy, R. M., M. Karplus, and J. A. McCammon. 1980. Molecular dynamics studies of NMR relaxation in proteins. *Biophys. J.* 32:628–630.
25. Levy, R. M., M. Karplus, and J. A. McCammon. 1981. Increase of ^{13}C NMR relaxation times in proteins due to picosecond motional averaging. *J. Am. Chem. Soc.* 103:994–996.
26. Abragham, A. 1978. The Principles of Nuclear Magnetism. Oxford University Press, London. 1–593.
27. Rowan, R., J. A. McCammon, and B. D. Sykes. 1975. A study of the distances obtained from nuclear magnetic resonance nuclear Overhauser effect and relaxation time measurements in organic structure determination. *J. Am. Chem. Soc.* 96:4773–4780.
28. Hull, W. H. 1975. Ph.D. Dissertation, Harvard University, Cambridge, MA.
29. Tropp, J. 1980. Dipolar relaxation and nuclear Overhauser effects in nonrigid molecules: the effect of fluctuating internuclear distances. *J. Chem. Phys.* 72:6035–6043.
30. Karplus, M., and J. A. McCammon. 1979. Protein structural fluctuations during a period of 100 ps. *Nature (Lond.).* 277:578–579.
31. McCammon, J. A., B. Gelin, and M. Karplus. 1977. The dynamics of folded proteins. *Nature (Lond.)* 267:325–326.
32. McCammon, J. A., P. G. Wolynes, and M. Karplus. 1979. Picosecond dynamics of tyrosine side chains in proteins. *Biochemistry.* 18:927–942.
33. Wallach, D. 1967. Effect of internal rotation on angular correlation functions. *J. Chem. Phys.* 47:5258–5264.
34. Levy, R. M., M. Karplus, and P. G. Wolynes. 1981. NMR relaxation parameters in molecules with internal motion: exact Langevin trajectory results compared with simplified relaxation models. *J. Am. Chem. Soc.* 103:5998–6011.
35. Wittebort, R. J., and A. Szabo. 1978. Theory of NMR relaxation in macromolecules: restricted diffusion and jump models for multiple internal rotations in amino acid side chains. *J. Chem. Phys.* 69:1722–1736
36. Brink, D. M., and G. R. Satchler. 1971. Angular momentum. Oxford University Press. London. 1–160.
37. Lipari, G., and A. Szabo. 1981. A model-free approach to the interpretation of NMR relaxation in macromolecules. *Biophys. J. (Abstr.)* 33:307 *a.*
38. Bocian, D. F., and S. I. Chan. 1979. NMR studies of membrane structure and dynamics. *Annu. Rev. Phys. Chem.* 29:307–335.
39. Diesenhofer, J., and W. Steigemann. 1975. Crystallographic refinement of the structure of bovine pancreatic trypsin inhibitor at 1.5 Å resolution. *Acta. Crystallogr. Sect. B.* 31:238–244.
40. McCammon, J. A., and M. Karplus. 1980. Simulation of protein dynamics. *Ann. Rev. Phys. Chem.* 31:29–46.
41. Wagner, G., and K. Wüthrich. 1978. Dynamic model of globular protein conformations based on NMR studies in solution. *Nature (Lond.).* 275:247–248.
42. McCammon, J. A., and M. Karplus. 1979. Dynamics of activated processes in globular proteins. *Proc. Natl. Acad. Sci.* 76:3585–3589.